Arabian Journal of Chemistry (2015) xxx, xxx–xxx

King Saud University

Arabian Journal of Chemistry

www.ksu.edu.sa
www.sciencedirect.com

ORIGINAL ARTICLE

Influence of pravastatin chitosan nanoparticles on erythrocytes cholesterol and redox homeostasis: An *in vitro* study

Gamaleldin I. Harisa [a,c,*], Mohamed M. Badran [b,d], Sabry M. Attia [e], Fars K. Alanazi [a], Gamal A. Shazly [b,f]

[a] *Kayyali Chair for Pharmaceutical Industry, Department of Pharmaceutics, College of Pharmacy, King Saud University, P.O. Box 2457, Riyadh 11451, Saudi Arabia*
[b] *Department of Pharmaceutics, College of Pharmacy, King Saud University, P.O. Box 2457, Riyadh 11451, Saudi Arabia*
[c] *Department of Biochemistry, College of Pharmacy, Al-Azhar University (Boys), Nasr City, Cairo, Egypt*
[d] *Department of Pharmaceutics, Faculty of Pharmacy, Al-Azhar University, Cairo, Egypt*
[e] *Department of Pharmacology and Toxicology, College of Pharmacy, King Saud University, Riyadh, Saudi Arabia*
[f] *Department of Industrial Pharmacy, Faculty of Pharmacy, Assiut University, Assiut, Egypt*

Received 3 September 2015; accepted 24 October 2015

KEYWORDS

Pravastatin;
Chitosan;
Nanoparticles;
Erythrocytes;
Oxidative stress

Abstract The objective of this study was to develop and characterize chitosan nanoparticles (CSNPs) to increase efficacy of pravastatin (PR) on erythrocytes redox status. CSNPs and PR loaded CSNPs (PRCSNPs) were prepared by ionic gelation method. The particle size, zeta potential, scanning electron microscopy (SEM), differential scanning calorimetry (DSC), Fourier-transform infrared (FTIR) and X-ray diffraction (XRD) were used to investigate physicochemical characters of the prepared nanoparticles. The present results revealed that CSNPs and PRCSNPs have nanosize about 90 nm with spherical shape, positive zeta potential and prolonged PR release. Moreover, DSC and FTIR indicated no chemical interactions between PR and CS. *In vitro* studies revealed that, erythrocyte uptake of PR from PRCSNPs was higher than free PR solution. Incubation of erythrocytes in high cholesterol plasma, hypercholesterolemia (HC), increases membrane cholesterol, erythrocyte hemolysis, oxidized glutathione (GSH), protein carbonyl (PCC), and malondialdeyhe (MDA). However, HC significantly decreases PR uptake by erythrocytes, superoxide dismutase (SOD), glutathione peroxidase (GPx) catalase (CAT) activities, reduced GSH and nitrite levels compared to control. By contrast, treatment of HC with PR plus CS as free drug or

* Corresponding author at: Department of Pharmaceutics, College of Pharmacy, King Saud University, P.O. Box 2457, Riyadh 11451, Saudi Arabia. Tel.: +966 546269544; fax: +966 (11) 4676295.
E-mail address: gamal.harisa@yahoo.com (G.I. Harisa).

Peer review under responsibility of King Saud University.

Production and hosting by Elsevier

http://dx.doi.org/10.1016/j.arabjc.2015.10.016

Please cite this article in press as: Harisa, G.I. et al., Influence of pravastatin chitosan nanoparticles on erythrocytes cholesterol and redox homeostasis: An *in vitro* study. Arabian Journal of Chemistry (2015), http://dx.doi.org/10.1016/j.arabjc.2015.10.016

nanostructure formula keeps the measured parameters at values near that of control. The effect of CSNPs and PRCSNPs on redox status of erythrocytes was more prominent than free drugs. In conclusion, PRCSNPs are promising drug carrier to deliver PR into erythrocytes, moreover, PRCSNPs possess promising characteristics with high biological safety for treatment of HC induced disruption of redox homeostasis.

1. Introduction

Under normal physiological conditions, erythrocytes have ability to release cardioprotective agents such as nitric oxide (NO), adenosine triphosphate (ATP) and scavenging reactive oxygen species (ROS) (Minetti et al., 2007; Cortese-Krott and Kelm, 2014). However, under pathological conditions, erythrocytes become as a source of ROS and lose their cardioprotective potential (Minetti et al., 2007; Eligini et al., 2013). For example, in hypercholesterolemia (HC), cholesterol crystallization in cell membrane is increased and this behavior disrupts redox homeostasis (Mason et al., 2004; Uydu et al., 2012; Tziakas et al., 2009). In such cases, erythrocytes lose antioxidant power by decreasing activity of antioxidant enzymes and decrease glutathione (GSH) content as major cellular antioxidant defense (Minetti et al., 2007). Therefore, they become enriched with oxidizable products of proteins, lipids and glutathione and are called oxidized erythrocytes (Oxi-Ery) (Minetti et al., 2007). Behavior of Oxi-Ery is similar to oxidized lipoproteins, so that Oxi-Ery takes in macrophages and triggers foam cells formation (Minetti et al., 2007; Lin et al., 2008; Tziakas et al., 2010; van Zwieten et al., 2012). Although most of research on HC deals with oxidized lipoproteins, few studies deal with Oxi-Ery (Franiak-Pietryga et al., 2009). Therefore, further studies are required to address this issue.

Statins are selective inhibitors of 3-hydroxy-3-methylglutaryl-CoA reductase (HMG-CoA reductase), a rate-limiting enzyme of the cholesterol biosynthetic pathway in the liver (Petyaev, 2015). Moreover, statins elicit peripheral effect through decreasing erythrocytes membrane cholesterol as well as preserve redox homeostasis (Forsyth et al., 2012; Uydu et al., 2012). Therefore, statins have many pleiotropic effects and been used in prevention and treatment of many diseases particularly cardiovascular disease. Several side effects such myopathies, memory impairment, neuropathies, elevated liver enzymes, general weakness and depression were reported for patients receiving high doses of statins (Petyaev, 2015). Statins bioavailability is low; this required increasing doses; however, increase-statin dosing may worsen their side effects during statin treatment (Petyaev, 2015). Therefore, further studies are required to enhance statins bioavailability such as novel formulation with vehicles that may increase statins efficacy (Anwar et al., 2011). It has been reported that chitosan nanoparticles (CSNPs) enhance bioavailability statins after oral administration (Anwar et al., 2011).

Nanocarriers-based drug deliveries are promising vehicle for targeted delivery, increase bioavailability, prolong action and increase cellular uptake of drug (Nam et al., 2009; Tao et al., 2011). Chitosan (CS) nanoparticles are biocompatible, biodegradable, drugs protection and innovative therapies (da Silva et al., 2015). Besides using of CS as drug delivery vehicle, it has biological effect such as cholesterol lowering and ROS scavenging effects (Tao et al., 2011). However, presence of free cationic group on CS induces binding with erythrocyte membranes, resulting in hemostasis, and rouleaux formation (Fernandes et al., 2008; Tsao et al., 2011; Yuan et al., 2011). Therefore, masking cationic groups reduces the harmful effect of CS on erythrocyte membranes (Ziemba et al., 2012). It was reported that, CSNPs prepared by ionic gelation method have low cationic properties, yet it still has cell binding capability (Nam et al., 2009; Tsao et al., 2011; Fan et al., 2012). Moreover, CSNPs have good erythrocyte compatibility, and act as potential vascular drug delivery system (Fan et al., 2012). Despite several studies documented the beneficial effects of nanoparticles, their effect on biological systems is still contradictory and further studies are required to confirm their beneficial effect or cancel harmful effects (Fröhlich, 2012; Narasimhan et al., 2014). In light of this, there has been a great interest influence of CSNPs and nano-statin on HC induced erythrocytes dysfunction.

Erythrocytes have been utilized as *in vitro* model to study physiological and pathophysiological situations (Fernandes et al., 2008). In particular, they are interest model to study membrane-related phenomena to better understanding of disease mechanisms, identification of new diagnostic and therapeutic approaches (Pasini et al., 2010). Despite several studies investigated the effect of statins and CS as cholesterol lowering agents, until now none of them addressed the effect of their combination as free form or nano-formula on erythrocytes. In this study, benefits of pravastatin (PR) and CS as hypocholesterolemic combination were investigated using erythrocytes as a vitro cellular model. This was achieved through preparation and characterization of CSNPs and PR loaded chitosan nanoparticles (PRCSNPs), moreover, the effect of these nanoparticles on HC induced erythrocytes cholesterol inclusion, oxidative status and hemolysis were investigated in comparison with free PR plus CS, an attempt to elucidate PRCSNPs biocompatibility and investigate their effect on erythrocyte redox status in HC situation.

2. Materials and methods

2.1. Materials and equipment

Pravastatin (PR) was purchased from Riyadh Pharma, Riyadh, Saudi Arabia. Sodium tripolyphosphate (TPP) and glacial acetic acid were obtained from BDH, UK. Low molecular weight chitosan, water-soluble cholesterol, tetraethoxypropane, GSH, glutathione oxidized (GSSG), O-pthalaldehyde (OPT), N-ethyl maleimide (NEM), and thiobarbituric acid (TBA) were obtained from Sigma–Aldrich

Please cite this article in press as: Harisa, G.I. et al., Influence of pravastatin chitosan nanoparticles on erythrocytes cholesterol and redox homeostasis: An *in vitro* study. Arabian Journal of Chemistry (2015), http://dx.doi.org/10.1016/j.arabjc.2015.10.016

(St. Louis, MO, USA). Trichloroacetic acid (TCA) was purchased from (Merck Germany), 2,4-Dinitrophenylhydrazine from (BDH Chemical Ltd Poole UK) and guanidine hydrochloride from Winlab UK. All other chemicals used were of reagent grade. The following equipments used in this study include Hettich EBA 20 Centrifuge (Germany), Ultra Centrifuge (Beckman Coulter, Pasadena, CA), Genesys10S UV–Vis spectrophotometer (USA) and Ultra Performance Liquid Chromatography (UPLC). Moreover, Zetasizer Nano ZS (Malvern Instruments, Malvern, UK), Wide-angle X-ray diffractometer (XRD, Rigaku Ultima IV, Tokyo, Japan), FT-IR spectrophotometer (FT-IR Nicolet-380, Thermo Fisher Scientific, Madison, USA) and A JEOL JSM-6380 LA scanning electron microscope (SEM) (Jeol Ltd., Tokyo, Japan) were used in used in this study.

2.2. Preparation and characterization of CSNPs and PRCSNPs

CSNPs and PRCSNPs were prepared by ionic gelation method using CS (3% w/w) and TPP (1% w/w) based on our previous study (Harisa et al., 2015). Briefly, TPP solution was added dropwise to 0.5 w/v of acidic solution of CS under continuous magnetic stirring at room temperature. CSNPs were formed spontaneously by interaction between negative groups of TPP and positively charged amino groups of CS. Then, CSNPs were sonicated for 3 min in order to break any aggregations and reduce particle size. The particle size, polydispersity index (PDI) and zeta potential (ZP) of CSNPs were measured by Zetasizer Nano ZS (Malvern Instruments, Malvern, UK) based on dynamic light scattering (DLS) technique. The entrapment efficiency and drug loading were calculated after centrifugation at 16,000 rpm for a period of 30 min and the amount of PR in supernatants was determined using UPLC. The CSNPs were freeze-dried and stored at 5 °C; the surface morphology of nanoparticles was investigated by SEM. The possible chemical interaction and the physical state of nanoparticles were determined by FTIR and X ray analysis, respectively (Hamidi et al., 2011).

2.3. Experimental design

In this study blood sample was obtained from apparent healthy, male volunteer aged 45 years. Inclusion criteria were based on normal plasma total cholesterol (150 mg mg/dL); however, exclusion criteria are physical inactivity, bad dietary habit, smoking, obesity, diabetes and other diseases. Blood sample (50 ml) was drawn by venipuncture into heparinized test tubes. Plasma samples were separated by centrifugation at 3000 rpm, and the buffy coat on top of cells was removed. Next, erythrocytes were gently washed 3 times with an equal volume of phosphate buffered saline (pH 7.5), following by further centrifugation and supernatant was discarded and cells were separated. Plasma samples were mixed with water-soluble cholesterol hereafter referred to as cholesterol-enriched plasma (HC) (550 mg/dL) (Kanakaraj and Singh, 1989). HC was confirmed by determination of cholesterol level using cholesterol oxidase method by a commercially available kit (Randox Laboratories, Crumlin, UK). Washed erythrocytes were *in vitro* mixed with normal plasma (150 mg/dL) and HC plasma (550 mg/dL) and treated with tested substances, as well as classified into six groups as follows:

Group 1: washed erythrocytes were suspended in normocholesterolemic plasma, referred as normal control (NC).
Group 2: washed erythrocytes were suspended in normal plasma plus a combination of PR (90 μM) (Broncel et al., 2007), and CS (1 mg/ml) (Fernandes et al., 2008), this group referred as normal control treated with PR plus CS, (NC + PR + CS group).
Group3: erythrocytes were suspended in HC plasma, and referred as (HC group) (Kanakaraj and Singh, 1989).
Group 4: erythrocytes were suspended in HC and treated with a combination of PR and CS, referred as HC treated with PR plus CS (HC + PR + CS group).
Group 5: erythrocytes were suspended in HC and treated with CSNPs (HC + CSNPs group) (Fan et al., 2012).
Group 6: erythrocytes were suspended in HC and treated with PRCSNPs (HC + PRCSNPs group).

All groups were incubated at 37 °C for 24 h, afterward samples were utilized by the following investigations. The protocol for this study conformed to the guidelines of the Institutional Ethical Committee.

2.3.1. Determination of PR erythrocytes uptake

Erythrocytes were incubated with normal plasma as normal control (NC) groups and with HC plasma as (HC) groups. Next the groups were treated with PR or with PRCSNPs as following groups 1: NC + PR, groups 2: NC + PRCSNPs, groups 3: HC + PR, and groups 4: HC + PRCSNPs, all group were incubated for 24 h at 37 °C. Then, uptake of PR by erythrocytes from PR solution and PRCSNPs was determined by calculation of the difference between initial and final PR concentrations in plasma at the start of the experiment and after 24 h incubation time with erythrocytes. PR was extracted from plasma by methanol. The method was performed on acquity® UPLC system, acquity® UPLC BEH C_{18} column (2.1 mm × 50 mm, 1.7 μm). The mobile phase was a mixture of 0.25% formic acid in distilled water and acetonitrile (65:35, v/v), with flow rate of 0.5 mL/min and injection volume was one μL. Photodiode array (PDA) detector was set to acquire 3D data from 210 to 280 nm while the 2D channel was recording at 237 nm, and the column temperature was kept at 50 °C while sample temperature was kept ambient. Method was validated and found to be linear, selective, precise and accurate as per FDA guidelines with low limit of detection 0.1 μg/mL and low limit of quantitation 0.5 μg/mL (Abdel-Hamid et al., 2012).

2.3.2. Determination of erythrocytes cholesterol inclusion

The cholesterol inclusion into erythrocyte was determined as following. Erythrocytes were incubated with HC, after 24 h incubation time, plasma samples were separated from erythrocytes, and initial and final cholesterol levels were determined by the cholesterol oxidase method using commercially available kits (Randox Laboratories, Crumlin, England). The percent of cholesterol inclusion (CI) on erythrocytes was calculated as follows.

$$\mathrm{CI}\% = \frac{\mathrm{CH\ conc.}_{\mathrm{Intial}} - \mathrm{CH\ conc.}_{\mathrm{Final}}}{\mathrm{CH\ conc.}_{\mathrm{Intial}}} \times 100$$

2.3.3. Determination of erythrocytes membrane cholesterol

Erythrocytes membrane cholesterol was extracted from hemolyzed cells using the procedure of Rose and Oklander (1965), in which lipids are extracted from an aliquot of erythrocyte membrane suspension with chloroform-isopropanol (7:11, v/v). Cholesterol was measured using cholesterol oxidase method using commercially available kits (Randox Laboratories, Crumlin, England).

2.3.4. Determination of erythrocytes membrane phospholipids

Phospholipid contents were determined as inorganic phosphorus by the following, 2 ml of chloroform extract was transferred to a clean Pyrex glass tube, and the solvent was completely evaporated. After addition of 0.2 ml perchloric acid (70%), the tubes were placed in a heating block at 180 °C until the yellow color was disappeared. Subsequently, 1 ml of distilled water, 150 μl of 2.5% (w/v) ammonium molybdate and 150 μl of 10% (w/v) ascorbic acid were added. All tubes were kept in boiling water for 5 min and the extent of the blue color was read spectrophotometrically at 800 nm (Rouser et al., 1970).

2.3.5. Assay of erythrocyte antioxidant enzymes

Erythrocyte catalase (CAT) activity was determined in erythrocyte lysate using the OxiSelect™ catalase activity assay (Cell Biolabs, San Diego, CA, USA). The CAT degrades H_2O_2 to water and molecular oxygen, and the amount of degraded H_2O_2 is proportional to the enzyme activity. The color change of the reaction mixture was measured spectrophotometrically at 520 nm. The CAT activity was calculated using a calibration curve.

Glutathione peroxidase (GPx) activity was measured in hemolysate by commercial RANSEL™ assay Kit (Randox Laboratories, Crumlin, UK). The GPx activity was assessed by measuring the decrease in absorbance at 340 nm.

SOD activity in the diluted lysate was measured using the commercial RANSOD™ assay (Randox Laboratories, Crumlin, UK). This method employs xanthine and xanthine oxidase (XOD) to generate superoxide radicals which react with 2-(4-iodophenyl)-3-(4-nitrophenol)-5-phenyltetrazolium chloride to form a red formazan dye. The absorbance was determined spectrophotometrically at a wavelength of 505 nm. The assay procedures were performed following the manufacturer's assay procedure. CAT, GPx and SOD were expressed as U/g Hb. Hemoglobin was measured in the whole blood sample by standard laboratory method.

2.3.6. Assay of erythrocyte glutathione

Reduced glutathione (GSH)/Oxidized glutathione (GSSG) contents of erythrocytes were measured using the method of Hissin and Hilf (1976), using O-phthalaldehyde (OPT), which forms a fluorescent derivative with GSH. Briefly, 0.2 mL erythrocyte pellet was diluted with 0.8 mL distilled water and proteins precipitated by addition of 1 mL of 10% trichloroacetic acid (TCA). The supernatant was used for GSH and GSSG assays. For GSH assay, 4 mL of reaction mixture consisted of 3.25 mL phosphate–EDTA buffer (0.1 M, pH 8.0), 0.25 mL OPT (1 mg/mL methanol) and 0.5 mL supernatant. The fluorescence of the GSH-OPT adduct was measured after 15 min using excitation and emission wavelengths of 350 and 450 nm, respectively.

For GSSG assay, N-ethyl maleimide (NEM) was used to inhibit the oxidation of GSH to GSSG during the estimation procedures, allowing the formation of a stable complex with GSH. After incubation of 0.5 mL of supernatant with 0.2 mL NEM (0.04 M) for 30 min, GSSG was measured using the same steps as the GSH assay, but using 0.1 N NaOH as a diluent instead of phosphate–EDTA buffer. The quantifications of GSH and GSSG were calculated using standard GSH and GSSG fluorescence and expressed as μmol/g hemoglobin. The ratio of GSSG and GSH was calculated by specific values in the samples.

2.3.7. Assay of erythrocytes protein carbonyl

The total protein carbonyl content (PCC) was determined in hemolysate as index of protein oxidation by a spectrophotometric method as described by Levine et al. (1994). The proteins were precipitated from hemolysate by addition of 10% TCA. The precipitate was resuspended in 1.0 mL of 2 M HCl for the blank control, or in 2 M HCl containing 2% 2,4-dinitrophenyl hydrazine for the test samples. After incubation for 1 h at 37 °C, protein samples were washed with alcohol/ethyl acetate mixture and precipitated again by the addition of 10% TCA. The precipitated protein was dissolved in 6 M guanidine hydrochloride solution and the absorbance was measured at 370 nm. The molar extinction coefficient of $22 \times 103\ M^{-1}\text{-}cm^{-1}$ was used for calculating the PCC level and expressed as nM of carbonyls formed per mg protein. The total protein content was determined according to Lowry et al. (1951), using bovine serum albumin as standard.

2.3.8. Assay of erythrocytes malondialdehyde

The concentration of malondialdehyde (MDA) in hemolysate, an index of lipid peroxidation, was determined spectrophotometrically (Ohkawa et al., 1979). A mixture of 200 μL of 8% sodium dodecyl sulfate, 200 μL of 0.9% thiobarbituric acid, and 1.5 mL of 20% acetic acid was added to a 200 μL supernatant of hemolysate and 1.9 mL of distilled water was used to make the volume up to 4 mL. After boiling for 1 h, the mixture was cooled and 5 mL of *n*-butanol and pyridine (15:1) solution was added. The mixture was centrifuged at 5000 rpm for 15 min and the absorbance was measured at 532 nm. MDA levels were calculated using tetraethoxypropane as standard.

2.3.9. Assay of erythrocyte nitrite

Nitrite was determined as index for NO production, erythrocytes were hemolysed by addition of ice-cold distilled water, and hemoglobin was precipitated by addition of cold ethanol and chloroform. After vortex, the mixture was centrifuged at 10,000 rpm for 10 min Carvalho et al. (2004). Nitrite concentrations were determined with Griess reagent according to the Griess Reagent Kit instructions (Cayman, Ann Arbor, USA). Firstly, nitrate was reduced to nitrite by nitrate reductase as described by Green et al. (1982), and 300 hundred μL of plasma was deproteinized by adding 600 μL of 75 mM $ZnSO_4$ solution. The mixture was stirred, and centrifuged at 10,000 rpm for 5 min at ambient temperature. Then 100 μL of supernatants was added to 40 μL of nitrate reductase (20 mU), 50 μL of FAD (5 mM), 10 μL of NADPH (0.6 mM), and 250 μL of phosphate buffer (50 mM). The mixtures were incubated for 1 h at 37 C, and then 150 μL of the

Please cite this article in press as: Harisa, G.I. et al., Influence of pravastatin chitosan nanoparticles on erythrocytes cholesterol and redox homeostasis: An *in vitro* study. Arabian Journal of Chemistry (2015), http://dx.doi.org/10.1016/j.arabjc.2015.10.016

mixture was added to 450 μL of Griess reagent and incubated in the dark place for 30 min at room temperature. Absorbance was measured at 545 nm; the nitrite levels were calculated from sodium nitrite standard curve and expressed in μM.

2.3.10. Assay of erythrocyte hemolysis

Osmotic fragility behavior of erythrocytes was determined as a measure of membrane integrity by the method of Parpart et al. (1947). The hemolysis percent regarding NaCl solution was determined as following. Firstly, 25 μl of erythrocyte from all studied groups was added to a series of 2.5 ml saline solutions (0.0–0.9% of NaCl) in test tubes. After gentle mixing and standing for 15 min at room temperature, the samples were centrifuged at 1500 rpm for 5 min then; absorbance of released hemoglobin was measured at 540 nm. Last, hemolysis was calculated as a percent from complete hemolysed samples represented as 100% hemolysis.

2.4. Statistical analysis

The statistical differences between groups were analyzed by one way ANOVA followed by TUKEY Kramer multiple comparison test, using GraphPad Prism Software v 5.01. The values at $P < 0.05$ were chosen as statistically significant.

3. Results

In the present study, PR loaded CSNPs were successfully prepared by ionic gelation method at ratio 3:1 for CS and TPP, respectively. The surface morphologies of CSNPs and PRCSNPs were shown in Fig. 1A and B. It was observed that nanoparticles were in spherical shape and their surfaces appeared smooth with a narrow size of distribution. The prepared CSNPs and PRCSNPs showed a unimodal size distribution (Fig. 1C and D), with nano size of 86.11 ± 3.76 and 91.23 ± 5.21 nm for CSNPs and PRCSNPs, respectively. A PDI values for loaded and unloaded nanoparticles are less than 0.3, which indicated homogeneity in particle size distribution. Moreover, both CSNPs and PRCSNPs exhibited a positive ZP. These results indicated that the nanoparticles were prepared successfully in terms of morphology and the uniform size distribution.

In addition, one of the significant parameters to be considered in CSNPs formulations is to get sufficient drug loading. As seen in Table. 1, the entrapment efficiency and drug loading of PR were 57.84 ± 2.45, and 23.61 ± 0.32 respectively. The loading of drug was improved by nanoparticle formulation. Regarding the nanoparticles stability, there were no detectable changes in color, odor, or transparency. In addition, neither CSNPs nor PRCSNPs did not show significant change in their

Table 1 The composition and characterization of CSNPs and PR loaded CSNPs (PRCSNPs).

Parameters	CSNPs	PRCSNPs
CS/TPP ratio	3:1	3:1
Particle size (nm)	86.11 ± 3.76	91.23 ± 5.21
Polydispersity index	0.245 ± 0.04	0.221 ± 0.02
Zeta potential (mV)	20.22 ± 3.35	17.21 ± 4.90
Entrapment efficiency (%)	–	57.84 ± 2.45
Drug loading (%)	–	23.61 ± 0.32
Drug release 48 h (%)	–	78.12 ± 4.81

Results were represented as M ± SD, ($N = 3$).

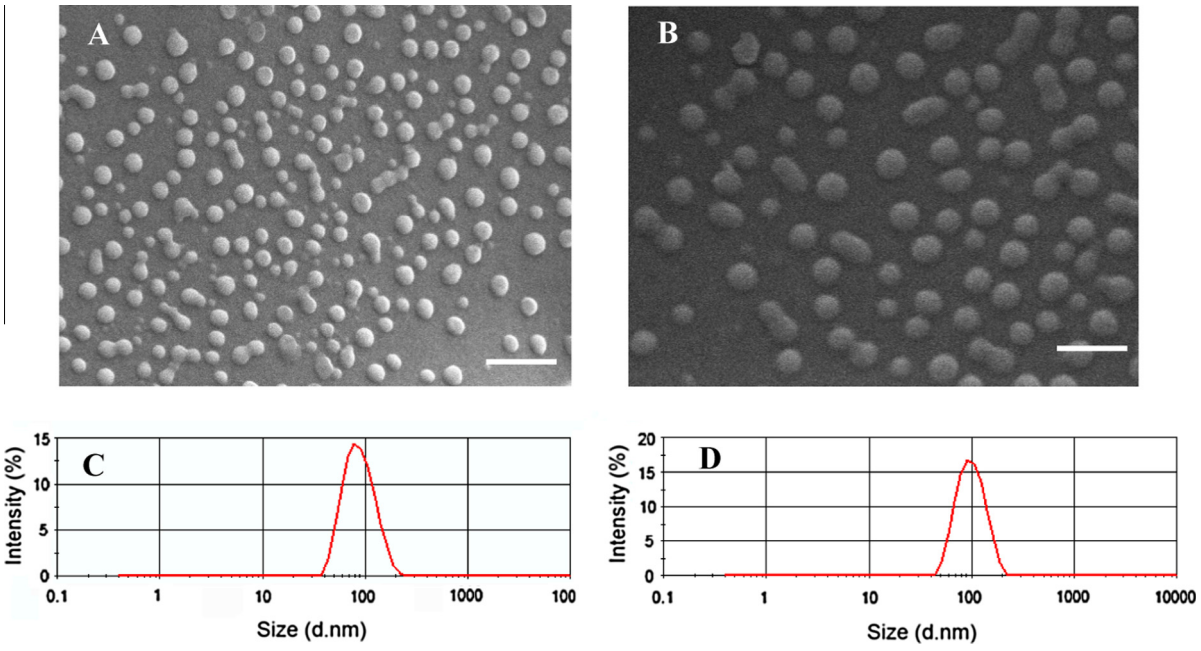

Figure 1 SEM images of plain CSNPs (A); PRCSNPs (B); particle size analysis of CSNPs (C) and PRCSNPs (D). Bar = 100 nm. This figure represents the micrograph of CSNPs (A) and PRCSNPs (B) at optimal conditions. The nanoparticles showed a spherical shape and had a narrow particle size distribution. The average of particle sizes was measured using dynamic light scattering (DLS). C displays DLS of CSNPs, however D displays PRCSNPs.

particle size and PDI upon storage for 1 month at 4 °C. In order to evaluate whether the PR undergoes chemical or physical changes or not when it is prepared in nanoparticles formulations, DSC, FTIR and XRD were examined. DSC was done to see the thermal behavior and crystallinity of PR after loading to CSNPs Fig. 2. DSC thermogram of PR showed a sharp melting peak at 175 °C. There were no thermal peaks for PRCSNPs that are related to melting point of PR. This could be attributed to the incorporation of PR in CS polymer matrices of the obtained nanoparticles. Moreover, FTIR spectroscopy was used to study the chemical interaction between PR and CS Fig. 3. The present results revealed the absence of interactions between PR and CS. The physical state of the materials was investigated by using XRD. The characteristic XRD spectra of pure drug (PR) and PR loaded CSNPs are presented in Fig. 4. The results of XRD experiment indicated that there are no appearance peaks of PR crystals. These results proved that PR had been added into the CS matrix in amorphous. PR release from PRCSNPs in phosphate buffered saline pH 7.4 at 37 °C, showed a biphasic pattern with an initial burst drug release followed by sustained release up 48 h.

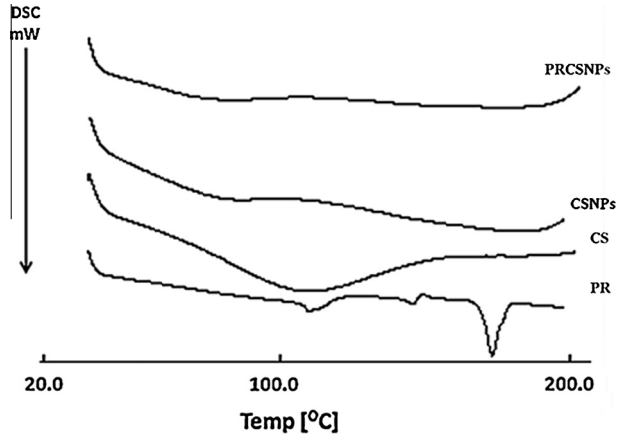

Figure 2 Differential scanning calorimetry (DSC) of PR, CS, CSNPS as well as PRCSNPs.

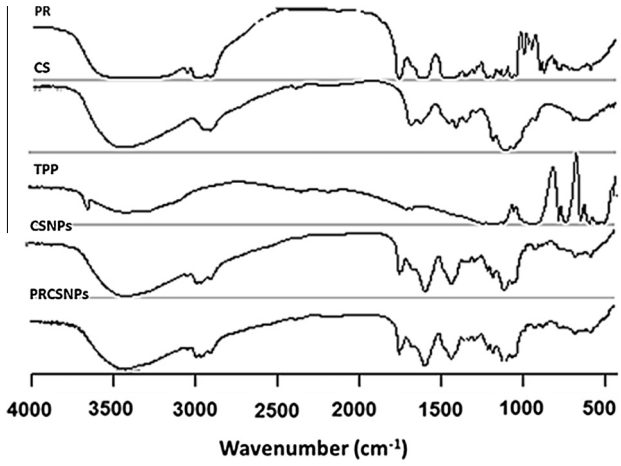

Figure 3 Fourier-transform infrared (FTIR) spectra of PR, CS, TPP, CSNPs and PRCSNPs.

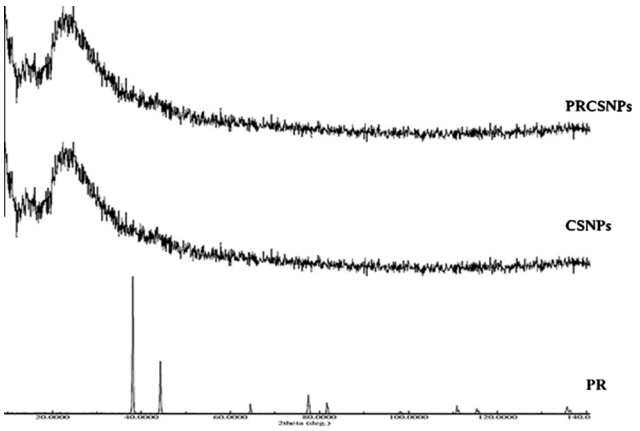

Figure 4 XRD patterns of PR, CSNPs and PRCSNPs.

The rapid PR releasing was mostly due to the nanoparticles surface drugs, which could simply diffuse in the first 6 h. The slow release could be caused by the diffusion of the drug from the CSNP matrix following by the degradation of the polymer up 48 h. The experiments were achieved in triplicate. The release of PR from PRCSNPs showed 78.12 ± 4.81% after 48 h (Table 1 and Fig. 5).

In the current work, the uptake of PR from PRCSNPs by erythrocytes was significantly higher than the uptake of free PR (control). However, cellular uptake of PR from the control and PRCSNPs was decreased in the presence of HC; these results were annotated in Fig. 6. Moreover, incubation of erythrocytes with HC induced a significant increase of cholesterol loading into erythrocyte membrane as compared to control ones ($P \leqslant 0.05$.). On the other hand, treatment with PR plus CS, CSNPs, or PRCSNPs significantly decreased cholesterol loading into erythrocyte membrane compared to HC group, Fig. 7 displayed these results.

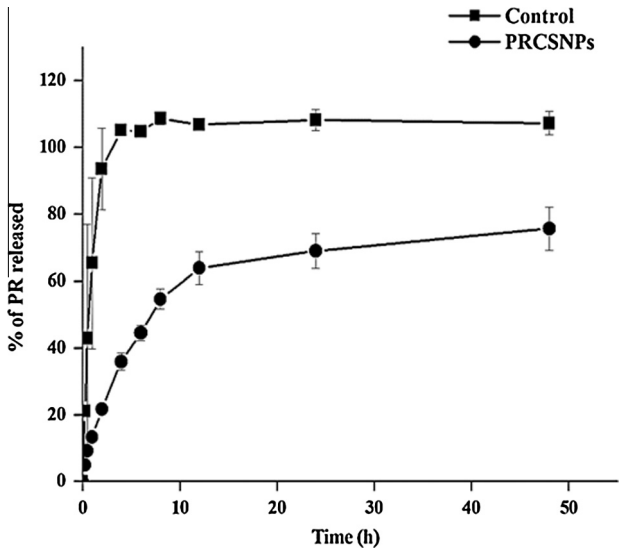

Figure 5 In vitro releasing profile of control PR and PRCSNPs in phosphate buffered saline (PBS) of pH 7.4 at 37 °C. Results were represented as M ± SD, ($N = 3$).

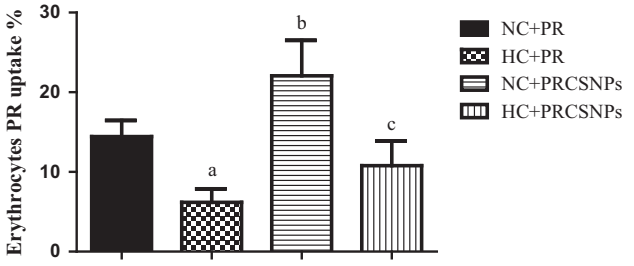

Figure 6 Cellular uptake of PR from free solution and CSNPs by erythrocytes incubated with normal plasma and HC plasma. One-way analysis of variance used for data analysis; Tukey posttest used to determine the statistical differences between groups. Results were represented as Mean ± SD, ($N = 6$). a, significant decrease from NC, b, significant increase from NC and HC incubated with free PR, c, significant increase from incubated with free PR. $P \leqslant 0.05$.

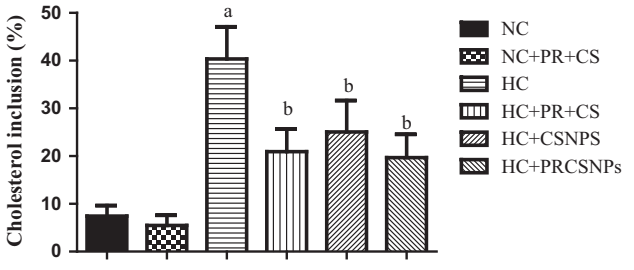

Figure 7 Effect of PR plus CS, CSNPs, and PRCSNPS on percent of cholesterol inclusion into erythrocytes membrane incubated with HC plasma compared to normal control. One-way analysis of variance used for data analysis; Tukey posttest used to determine the statistical differences between groups. Results were represented as Mean ± SD, ($N = 6$). Superscript letters indicated when significant differences observed from either control group or HC group. a; significantly decrease from control, b; significantly increase from control, $P \leqslant 0.05$.

The present results reveal that, exposure of erythrocytes to HC induced a significant increase of membrane cholesterol/phospholipids ratio (CH/PL) and erythrocytes hemolysis compared to control ($P \leqslant 0.05$). However, incubation of erythrocytes with HC in the presence of PR plus CS, CSNPS, or PRCSNPs preserved CH/PL ratio near and hemolysis that of control ones. Table 2 displayed the effect of HC and tested formulations on erythrocyte membrane CH/PL and hemolysis percent.

Table 3 showed that, activity of SOD, GPx, CAT as well as SOD/CAT and SOD/GPx ratios of control erythrocyte group and incubated erythrocyte groups with PR plus CS as free drug or as nanoparticle formulations. These data indicated that, the treatment of erythrocytes with a combination of PR and CS preserves activity of antioxidant enzymes and their ratios at value near that of control one. However, a significant ($P \leqslant 0.05$) decrease in SOD, GPx, and CAT activities was observed in erythrocytes incubated with HC compared to control. SOD/CAT and SOD/GPx ratios were significantly increased by exposure to HC plasma. On the other side, treatment of HC group with a combination of PR plus CS, CSNPs, or PRCSNPs ameliorates activity of measured enzymes and their ratios compared to HC group. There is no significant difference between PR plus CS and PRCSNPs.

In the present results, GSH levels and GSH/GSSG ratio markedly decreased in HC treated group compared to normal control cells ($P \leqslant 0.05$). However, GSSG, MDA and PCC were significantly increased by HC exposure compared to control cells ($P \leqslant 0.05$). Treatment of HC group with free PR plus CS or as nanoparticles kept GSH, GSSG, MDA and PCC at values similar to control group. With respect to nitrite level, HC exposure caused a significant decrease of nitrite level compared to the control ($P \leqslant 0.05$). However, incubation of erythrocytes with either free drugs or nanoparticles elicits marked increase of nitrite level compared to HC treated cells ($P \leqslant 0.05$). The effect of CSNPs and PRCSNP on GSH, GSSG, PCC, MDA and nitrite was pronounced (18–31%) than free CS plus PR. Table 4 showed the statistical data corresponding to these results.

4. Discussion

The integration of nanotechnology with biology has led to development of drug nanocarriers that increase drug bioavailability, enhance intracellular delivery, and sustained release of drugs (Wang et al., 2014). Nanotechnology was applied to deliver drugs to treat several chronic diseases (da Silva, 2015). Despite Psarros et al. (2012) reported that nanotechnology elicits beneficial effect in treatment of vascular diseases, further studies are required to confirm this assumption.

In the present study, the prepared nanoparticles have nanosize as well as good entrapment efficiency and drug release. These observations concur with earlier studies, demonstrated that statins could be prepared as nanoparticles with acceptable physicochemical properties (Zhang et al., 2010; Anwar et al., 2011; Tiwari and Pathak, 2011; Harisa et al., 2015; da Silva et al., 2015). Herein, erythrocyte uptake of PR from PRCSNPs was higher than free PR solution. This effect may attribute to positive ZP of PRCSNPs that enhanced PR entry into erythrocytes. These findings are in agreement with several studies, reported that nanocarriers with positive ZP interact with negatively charged cells membrane (Bankapur et al., 2014). In addition, Alexis et al. (2008) indicated that positively charged nanocarriers have higher cellular uptake in comparison with neutral or negatively charged one. Additionally, passive transport may involve in nanocarriers uptake by erythrocyte (Bankapur et al., 2014). CSNPs bind to negatively charged cell membranes by an electrostatic interaction driven by its positively charged amino group (da Silva, 2015).

In HC conditions, erythrocytes are floating in cholesterol enriched medium, therefore free cholesterol molecules were trapped in erythrocyte membrane (Franiak-Pietryga et al., 2009). In this study, HC increased cholesterol inclusion on erythrocytes, and these results are in agreement with our previous study and other studies (Harisa and Badran, 2015; Uydu et al., 2012). In contrary, the treatment with PR plus CS or their nanoparticles prevents the deposition of cholesterol into erythrocyte membranes. Similarly, Franiak-Pietryga et al. (2009) and Foryth et al. (2012) reported that statins decrease cholesterol content in erythrocyte membranes. Furthermore, Tsao et al. (2011), indicated that CS and CSNPs elicit cholesterol-lowering effect. The interaction between positively charged

Table 2 Effect of HC plasma with or without treatment on erythrocytes membrane cholesterol (CH), phospholipids (PL), CH/PL ratio and hemolysis percent compared to control group.

Parameters	NC	NC + PR + CS	HC	HC + PR + CS*	HC + CSNPs	HC + PRCSNPs
CH	415.0 ± 34.0	358.7 ± 42.3	593.3 ± 72.60[a]	368.8 ± 53.98[b]	387.8 ± 51.51[b]	372.7 ± 53.4[b]
PL	683.0 ± 103	681.5 ± 70.0	558.7 ± 112.6	575.0 ± 142.6	647.8 ± 102.9	674.0 ± 87.19
CH/PL	0.61 ± 0.03	0.53 ± 0.04	1.062 ± .41[a]	0.64 ± 0.09[b]	0.60 ± 0.14[b]	0.55 ± 0.06[b]
Hemolysis (%)	11.50 ± 1.12	5.45 ± 0.43	28.6 ± 3.71[a]	13.52 ± 0.97[b]	15.63 ± 1.63[b]	12.43 ± 1.34[b]

One-way analysis of variance used for data analysis; Tukey's posttest was used to determine the statistical differences between groups. Results were represented as M ± SD, ($N = 6$). Superscript letters indicated when significant differences were observed from either control group or HC group. a; Significantly increase from control, b; significantly decrease from HC, $P \leqslant 0.05$. Units; Erythrocyte cholesterol expressed as (μg/mg protein), while phospholipids were expressed as inorganic phosphate (μg/mg protein).

* Indicated that HC treated with free PR + CS as positive control compared to HC treated with PRCSNPs to show how using nanotechnology influences the biochemical measures.

Table 3 Effect of HC plasma with or without treatment on erythrocyte SOD, GPx and CAT and their ratios compared to control erythrocytes.

Parameters	NC	NC + PR + CS	HC	HC + PR + CS*	HC + CSNPs	HC + PRCSNPs
SOD	1292 ± 98.6	1488 ± 184	945.5 ± 83.8[a]	1207 ± 98.6[c]	1130 ± 105[c]	1251 ± 1106[c]
GPx	47.17 ± 4.04	55.77 ± 6.39	21.99 ± 4.20[a]	41.10 ± 4.91[c]	31.10 ± 2.93[c]	45.10 ± 5.93[c]
CAT	72.80 ± 8.00	82.50 ± 7.22	31.58 ± 3.10[a]	70.1 ± 5.22[c]	57.56 ± 4.96[c]	71.37 ± 6.48[c]
SOD/GPx	27.39 ± 3.83	26.68 ± 2.35	43.1 ± 5.46[b]	28.36 ± 3.10[d]	36.33 ± 2.68[d]	28.53 ± 2.83[d]
SOD/CAT	17.75 ± 1.88	18.04 ± 1.72	29.94 ± 3.24[b]	17.22 ± 1.67[d]	19.63 ± 2.33[d]	16.83 ± 1.39[d]

One-way analysis of variance used for data analysis; Tukey's posttest was used to determine the statistical differences between groups. Results were represented as M ± SD, ($N = 6$). Superscript letters indicated when significant differences were observed from either control group or HC group. a; significantly decrease from control, b; significantly increase from control, c; significantly higher than HC, d; significantly lower than HC, $P \leqslant 0.05$. Units; SOD, GPx and CAT were expressed as U/g Hb.

* Indicated that HC treated with free PR + CS as positive control compared to HC treated with PRCSNPs to show how using nanotechnology influences the biochemical measures.

Table 4 Effect of HC with or without tested agents on erythrocyte GSH, GSSG, GSH/GSSG ratio, MDA, PCC, and nitrite content compared to control erythrocytes.

Parameters	NC	NC + PR + CS	HC	HC + PR + CS*	HC + CSNPs	HC + PRCSNPs
GSH	17.41 ± 2.28	21.05 ± 1.98	8.976 ± 1.76[a]	13.77 ± 1.58[c]	14.98 ± 1.67[c]	16.69 ± 1.43[c]
GSSG	0.418 ± 0.21	0.380 ± .08	0.883 ± 0.30[b]	0.510 ± 0.06[c]	0.622 ± 0.14[d]	0.415 ± .08[d]
GSH/GSSG	42.65 ± 4.23	55.39 ± 8.01	10.17 ± 1.12[a]	30.92 ± 3.41[c]	24.80 ± 2.75[c]	36.40 ± 4.11[c]
MDA	13.24 ± 1.11	10.45 ± 1.10	28.45 ± 1.89[b]	17.71 ± 1.73[d]	21.19 ± 2.27[d]	14.57 ± 1.37[d]
PCC	1.93 ± 0.34	1.23 ± 0.21	6.24 ± 0.84[b]	2.94 ± .0.55[d]	3.23 ± 0.64[d]	2.02 ± 0.61[d]
Nitrite	581.8 ± 97.14	620.1 ± 98.47	298.3 ± 34.56[a]	543.6 ± 91.77[c]	530.4 ± 67.43[c]	565.0 ± 77.65[c]

Data were analyzed using one-way analysis of variance followed by Turkey's posttest to determine the statistical differences between groups. Results were represented as mean ± SD, ($N = 6$). Superscript letters indicated when significant differences observed from either control group or HC group. a; significantly decrease from control, b; significantly increase from control, c; significantly increase from HC group, d; significantly decreased from HC group, $P \leqslant 0.05$. Units; GSH and GSSG expressed as μM/g Hb MDA, μM; PCO, nM mg/protein and nitrite, μM.

* Indicated that HC treated with free PR + CS as positive control compared to HC treated with PRCSNPs to show how using nanotechnology influence the biochemical measures.

amino groups of CS and cholesterol may be contributed to cholesterol membrane inclusion (Xia et al., 2010). Therefore, Free PR and Cs combination as well as PRCSNPs treatment decreased cholesterol accumulation into an erythrocytes membrane.

In this work, GSH content, SOD, GPx, and CAT activities were decreasing by HC exposure; these findings confirmed that HC induced oxidative stress. Several studies demonstrated that the exposure of erythrocytes to HC produced depletion of antioxidant capacity (Devrim et al., 2008; Franiak-Pietryga et al., 2009; Aydin et al., 2009; Uydu et al., 2012). However, increase of SOD/CAT and SOD/GPx ratios, GSSG, PCO and MDA in erythrocytes exposed to HC attributed to enhancement ROS production that consumes antioxidant systems (Devrim et al., 2008; Aydin et al., 2009; Uydu et al., 2012; Ramírez-Zamora et al., 2013). Consequently, Oxi-Ery

is formed and rich with GSSG, oxidized lipids and proteins, therefore they interact with macrophages to produce foam cells that have a primary role in atherogenesis (Minetti et al., 2007; Franiak-Pietryga et al., 2009).

By contrast, treatment of erythrocytes with PR plus CS as free drug or in nanoparticles keeps the measured oxidative stress variable at values near that of control. Similarly, many studies demonstrated that statins and CS preserve antioxidant systems and inhibit HC induced oxidation of biomolecules (Franiak-Pietryga et al., 2009; Aydin et al., 2009; Uydu et al., 2012; Anandan et al., 2012; Anandan et al., 2013). In addition, Nasr et al. (2014), demonstrated that CSNPs have more powerful antioxidant compared to free CS. Likewise Wen et al. (2013) suggested that CSNPs are more effective against oxidative stress as compared to free CS. Therefore, CSNPs are promising drug carriers in antioxidant system (Yadav et al., 2012; Du et al., 2014). Herein, CSNPs and PRCSNPs treatment maintain antioxidant capacity of erythrocytes. This indicated that, construction of PR and CS in nanoparticles form not abolishes hypocholesterolemic and antioxidant activities. The insignificant difference between PR plus CS and PRCSNPs on antioxidant enzyme may be attributed to partial masking of CS amino or hydroxyl group of PR or delaying release of CS and PR from nanoparticles. Similarly, it has been demonstrated that nanoparticles and free drug elicit similar or improved biological effect (Kwak et al., 2015).

One of cardioprotective function of erythrocytes is regulation of nitric oxide (NO) homeostasis, therefore, impairment of erythrocytes NO production has been reported in cardiovascular diseases (Eligini, 2013). Herein, HC induced a significant decrease of NO production compared to the control. This attributes to HC impairs L-arginine active transport into cells and enhances ROS formation; therefore, NO production was decreased (Mason et al., 2004). In addition, Eligini et al. (2013) demonstrated that oxidative stress impaired NO pathway in erythrocytes. Moreover, Ramírez-Zamora et al. (2013) reported that ROS inhibits NO production. Conversely, the treatment of HC group with PR plus CS elicits marked increase of NO compared to HC. These results are similar to several studies, which reported that statins improve NO level (Harisa et al., 2012; Li and Forstermann, 2013). Moreover, Heeba et al. 2009 established that statins restore NO level. This may be due to ability of statins to decrease cellular cholesterol inclusion (Forsyth et al., 2012; Uydu et al., 2012). In addition, CS significantly increased NO levels (Ozcelik et al., 2014; Zhang et al., 2014). Moreover, it has been demonstrated that CSNPs enhance NO production (Pattani et al., 2009). This may be attributed to the presence of amino groups on CS that scavenges ROS.

The increase of cholesterol inclusion into erythrocytes membrane ratio decreases the membrane fluidity, and consequently, increased erythrocyte hemolysis. The hemolytic products of erythrocytes such as cholesterol, iron and oxidized hemoglobin are powerful damaging agents that increase risk of vascular damage (Tziakas et al., 2010). In the present study, the increase of erythrocyte hemolysis by HC exposures runs in parallel with observations documented in several earlier studies (Uydu et al., 2012). However, PR plus CS as free drug or in nanoparticle formulae decreased HC-induced erythrocytes hemolysis. These observations concur with earlier studies, which reported that statins are protective agents against erythrocyte hemolysis (Uydu et al., 2012; Harisa et al., 2012). Moreover, Anandan et al. (2013) indicated that CS has membrane-stabilizing property. Therefore, PR and CS are protective agents against erythrocytes hemolysis. The decrease of erythrocytes hemolysis by PRCSNPs indicated that safety of CSNPs and PRCSNPs on biological systems.

5. Conclusion

In conclusion, the prepared PRCSNPs have desired nanoparticle size, high entrapment efficiency and drug release. PR and CS are effective combination for treatment of HC induced erythrocytes cholesterol inclusion and disruption of redox homeostasis. PRCSNPs have similar activities in terms of cholesterol inclusion inhibition, decrease hemolysis and restoration of antioxidant activity to that of PR plus CS. However, their effect was pronounced on GSH, GSSG, PCC, MDA and nitrite. A relatively small sample size and lack of *in vivo* studies were the limitations of this study. Further large-scale *in vivo* studies are required to address this issue.

Acknowledgments

This Project was funded by the National Plan for Science, Technology and Innovation (MAARIFAH), King Abdulaziz City for Science and Technology, Saudi Arabia, Award Number (12-MED2563-02).

References

Abdel-Hamid, M., Ibrahim, M.F., Harisa, G.I., Alanazi, F.K., 2012. Ultra performance liquid chromatography determination ofpravastatin sodium in erythrocytes. Asian J. Chem. 24 (2), 584.

Alexis, F., Pridgen, E., Molnar, L.k., Farokhzad, O.C., 2008. Factors affecting the clearance and biodistribution of polymeric nanoparticles. Mole. Pharma. 5, 505–515.

Anandan, R., Ganesan, B., Obulesu, T., Mathew, S., Asha, K.K., Lakshmanan, P.T., Zynudheen, A.A., 2013. Antiaging effect of dietary chitosan supplementation on glutathione-dependent antioxidant system in young and aged rats. Cell Stress Chaperones. 18 (1), 121–125.

Anandan, R., Ganesan, B., Obulesu, T., Mathew, S., Kumar, R.S., Lakshmanan, P.T., Zynudheen, A.A., 2012. Dietary chitosan supplementation attenuates isoprenaline-induced oxidative stress in rat myocardium. Int. J. Biol. Macromol. 51 (5), 783–787.

Aydin, S., Uzun, H., Sozer, V., Altug, T., 2009. Effects of atorvastatin therapy on protein oxidation and oxidative DNA damage in hypercholesterolemic rabbits. Pharmacol. Res. 59 (4), 242–247.

Anwar, M., Warsi, M.H., Mallick, N., Akhter, S., Gahoi, S., Jain, G. K., Talegaonkar, S., Ahmad, F.J., Khar, R.K., 2011. Enhanced bioavailability of nano-sized chitosan-atorvastatin conjugate after oral administration to rats. Eur. J. Pharm. Sci. 44 (3), 241–249.

Bankapur, A., Barkur, S., Chidangil, S., Mathur, D., 2014. A micro-Raman study of live, single red blood cells (RBCs) treated with ANO3 nanoparticles. PLoS ONE 9 (7), e103493.

Broncel, M., Franiak, I., Koter-Michalak, M., Duchnowicz, P., Chojnowska-Jezierska, J., 2007. The comparison in vitro the effects of pravastatin and quercetin on the selected structural parameters of membrane erythrocytes from patients with hypercholesterolemia. Pol. Merkur. Lekarski. 22 (128), 112–116.

Carvalho, F.A., Mesquita, R., Martins-Silva, J., Saldanha, C., 2004. Acetylcholine and choline effects on erythrocyte nitrite and nitrate levels. J. Appl. Toxicol. 24 (6), 419–427.

Cortese-Krott, M.M., Kelm, M., 2014. Endothelial nitric oxide synthase in red blood cells: key to a new erythrocrine function. Redox Biol. 2, 251–258.

da Silva, S.B., Amorim, M., Fonte, P., Madureira, R., Ferreira, D., Pintado, M., Sarmento, B., 2015. Natural extracts into chitosan nanocarriers for rosmarinic acid drug delivery. Pharm. Biol. 53 (5), 642–652.

Devrim, E., Ergüder, I.B., Ozbek, H., Durak, I., 2008. High-cholesterol diet increases xanthine oxidase and decreases nitric oxide synthase activities in erythrocytes from rats. Nutr. Res. 28 (3), 212–215.

Du, L., Miao, X., Gao, Y., Jia, H., Liu, K., Liu, Y., 2014. The protective effects of Trolox-loaded chitosan nanoparticles against hypoxia-mediated cell apoptosis. Nanomedicine. 10 (7), 1411–1420.

Eligini, S., Porro, B., Lualdi, A., Squellerio, I., Veglia, F., Chiorino, E., Crisci, M., et al, 2013. Nitric oxide synthetic pathway in red blood cells is impaired in coronary artery disease. PLoS ONE 8 (8), e66945.

Fan, W., Yan, W., Xu, Z., Ni, H., 2012. Erythrocytes load of low molecular weight chitosan nanoparticles as a potential vascular drug delivery system. Colloids Surf. B Biointerfaces 95, 258–265 (Jun. 15).

Fernandes 1, J.C., Eaton, P., Nascimento, H., Belo, L., Rocha, S., Vitorino, R., Amado, F., Gomes, J., Santos-Silva, A., Pintado, M. E., Malcata, F.X., 2008. Effects of chitooligosaccharides on human red blood cell morphology and membrane protein structure. Biomacromolecules 9 (12), 3346–3352.

Franiak-Pietryga, I., Koter-Michalak, M., Broncel, M., Duchnowicz, P., Chojnowska-Jezierska, J., 2009. Anti-inflammatory and hypolipemic effects in vitro of simvastatin comparing to epicatechin in patients with type-2 hypercholesterolemia. Food Chem. Toxicol. 47 (2), 393–397.

Fröhlich, E., 2012. The role of surface charge in cellular uptake and cytotoxicity of medical nanoparticles. Int. J. Nanomedicine 7, 5577–5591.

Forsyth, A.M., Braunmüller, S., Wan, J., Franke, T., Stone, H.A., 2012. The effects of membrane cholesterol and simvastatin on red blood cell deformability and ATP release. Microvasc. Res. 83 (3), 347–351.

Green, L., Wagner, D., Glogowski, J., Skipper, P., Wishnok, J., Tannenbaum, S., 1982. Analysis of nitrate, nitrite and [15N] nitrate in biological fluids. Anal. Biochem. 126, 131–138.

Hamidi, M., Rafiei, P., Azadi, A., Mohammadi-Samani, S., 2011. Encapsulation of valproate-loaded hydrogel nanoparticles in intact human erythrocytes: a novel nano-cell composite for drug delivery. J. Pharm. Sci. 100 (5), 1702–1711.

Harisa, G.I. et al, 2015. Pravastatin chitosan nanogels-loaded erythrocytes as a new delivery strategy for targeting liver cancer. Saudi Pharm. J. http://dx.doi.org/10.1016/j.jsps.03.024.

Harisa, G.I., Alanazi, F.K., El-Bassat, R.A., Malik, A., Abdallah, G. M., 2012. Protective effect of pravastatin against mercury induced vascular cells damage: erythrocytes as surrogate markers. Environ. Toxicol. Pharmacol. 34 (2), 428–435.

Harisa, G.I., Badran, M.M., 2015. Simvastatin nanolipid carriers decreased hypercholesterolemia induced cholesterol inclusion and phosphatidylserine exposure on human erythrocytes. J. Mol. Liq. 208 (2015), 202–210.

Heeba, G., Moselhy, M.E., Hassan, M., Khalifa, M., Gryglewski, R., Malinski, T., 2009. Anti-atherogenic effect of statins: role of nitric oxide, peroxynitrite and haem oxygenase-1. Br. J. Pharmacol. 156, 1256–1266.

Hissin, P.J., Hilf, 1976. A fluorometric method for determination of oxidized and reduced glutathione in tissues. Anal. Biochem. 74, 214–226.

Kanakaraj, P., Singh, M., 1989. Influence of hypercholesterolemia on morphological and rheological characteristics of erythrocytes. Atherosclerosis 76 (2–3), 209–218.

Kwak, T.W., Do Jeong, H.K., Kang, D.H., 2015. Antitumor activity of vorinostat-incorporated nanoparticles against human cholangiocarcinoma cells. J. Nanobiotechnol. 13, 60.

Levine, R.L., Williams, J.A., Stadtman, E.R., Shacter, E., 1994. Carbonyl assays for determination of oxidatively modified proteins. Methods Enzymol. 233, 346–357.

Li, H., Förstermann, U., 2013. Uncoupling of endothelial NO synthase in atherosclerosis and vascular disease. Curr. Opin. Pharmacol. 13, 161–167.

Lin, H.L., Xu, X.S., Lu, H.X., Li, C.J., Tang, M.X., Sun, H.W., Zhang, Y., 2008. Pathological mechanisms of erythrocyte-induced vulnerability of atherosclerotic plaques. Med. Hypotheses. 70 (1), 105–108.

Lowry, O.H., Rosebrough, N.J., Farr, A.L., Randall, R.J., 1951. Protein measurement with the Folin phenol reagent. J. Biol. Chem. 193, 265–275.

Mason, R.P., Walter, M.F., Jacob, R.F., 2004. Effects of HMG-CoA reductase inhibitors on endothelial function: role of microdomains and oxidative stress. Circulation 109 (21 Suppl 1), II34–II41.

Minetti, M., Agati, L., Malorni, W., 2007. The microenvironment can shift erythrocytes from a friendly to a harmful behavior: pathogenetic implications for vascular diseases. Cardiovasc. Res. 75 (1), 21–28.

Nam, H.Y., Kwon, S.M., Chung, H., Lee, S.Y., Kwon, S.H., Jeon, H., Kim, Y., et al, 2009. Cellular uptake mechanism and intracellular fate of hydrophobically modified glycol chitosan nanoparticles. J. Control Release 135 (3), 259–267.

Narasimhan, G., de Alba-Aguayo, D.R., Mondragón-Flores, R., González-Pozos, S., Miranda-Saturnino, M.J., Sridharan, M., Rueda, A., 2014. Acute administration of chitosan nanoparticles increases Ca^{2+} leak in rat cardiomyocytes. J. Nano Res. 28, 29–38.

Nasr, M., Nafee, N., Saad, H., Kazem, A., 2014. Improved antitumor activity and reduced cardiotoxicity of epirubicin using hepatocyte-targeted nanoparticles combined with tocotrienols against hepatocellular carcinoma in mice. Eur. J. Pharm. Biopharm. 88 (1), 216–225.

Ohkawa, H., Ohishi, N., Yagi, K., 1979. Assay for lipid peroxides in animal tissues by thiobarbituric acid reaction. Anal. Biochem. 95, 351–358.

Ozcelik, E., Uslu, S., Burukoglu, D., Musmul, A., 2014. Chitosan and blueberry treatment induces arginase activity and inhibits nitric oxide production during acetaminophen-induced hepatotoxicity. Pharmacogn Mag. Apr 10 (Suppl 2), S217–S224.

Parpart, A.K., Lorenz, P.B., Parpart, E.R., Gregg, J.R., Chase, A.M., 1947. The osmotic resistance (fragility) of human red cells. J. Clin. Invest. 26 (4), 636–640.

Pasini, E.M., Lutz, H.U., Mann, M., Thomas, A.W., 2010. Red blood cell (RBC) membrane proteomics–Part I: Proteomics and RBC physiology. J. Proteomics. 73 (3), 403–420.

Pattani, A., Patravale, V.B., Panicker, L., Potdar, P.D., 2009. Immunological effects and membrane interactions of chitosan nanoparticles. Mol. Pharm. 6 (2), 345–352.

Petyaev, I.M., 2015. Improvement of hepatic bioavailability as a new step for the future of statin. Arch. Med. Sci. 11 (2), 406–410.

Psarros, C., Lee, R., Margaritis, M., Antoniades, C., 2012. Nanomedicine for the prevention, treatment and imaging of atherosclerosis. Maturitas 73 (1), 52–60.

Ramírez-Zamora, S., Méndez-Rodríguez, M.L., Olguín-Martínez, M., Sánchez-Sevilla, L., Quintana-Quintana, M., García-García, N., Hernández-Muñoz, R., 2013. Increased erythrocytes by-products of arginine catabolism are associated with hyperglycemia and could be involved in the pathogenesis of type 2 diabetes mellitus. PLoS ONE 8 (6), e66823, Jun 24.

Rose, H.G., Oklander, M., 1965. Improved procedure for the extraction of lipid from human erythrocytes. J. Lipid. Res. 6, 428–431.

Rouser, G., Fkeischer, S., Yamamoto, A., 1970. Two dimensional then layer chromatographic separation of polar lipids and determination of phospholipids by phosphorus analysis of spots. Lipids 5, 494–496.

Please cite this article in press as: Harisa, G.I. et al., Influence of pravastatin chitosan nanoparticles on erythrocytes cholesterol and redox homeostasis: An *in vitro* study. Arabian Journal of Chemistry (2015), http://dx.doi.org/10.1016/j.arabjc.2015.10.016

Tao, Yi, Zhang, Hongliang, Gao, Bing, Guo, Jiao, Hu, Yinming, Su, Zhengquan, 2011. Water-soluble chitosan nanoparticles inhibit hypercholesterolemia induced by feeding a high-fat diet in male sprague-dawley rats. J. Nanomater. 814606

Tiwari, R., Pathak, K., 2011. Nanostructured lipid carrier versus solid lipid nanoparticles of simvastatin: comparative analysis of characteristics, pharmacokinetics and tissue uptake. Int. J. Pharm. 415 (1-2), 232–243.

Tsao, C.T., Chang, C.H., Lin, Y.Y., Wu, M.F., Han, J.L., Hsieh, K. H., 2011. Kinetic study of acid depolymerization of chitosan and effects of low molecular weight chitosan on erythrocyte rouleaux formation. Carbohydr. Res. 346 (1), 94–102.

Tziakas, D.N., Chalikias, G.K., Stakos, D., Boudoulas, H., 2010. The role of red blood cells in the progression and instability of atherosclerotic plaque. Int. J Cardiol. 142 (1), 2–7.

Tziakas, D.N., Chalikias, G.K., Stakos, D., Tentes, I.K., Thomaidi, A., Chatzikyriakou, S., Mitrousi, et al, 2009. Statin use is associated with a significant reduction in cholesterol content of erythrocyte membranes. A novel pleiotropic effect? Cardiovasc. Drugs Ther. 23 (6), 471–480.

Uydu, H.A., Yıldırmış, S., Orem, C., Calapoglu, M., Alver, A., Kural, B., Orem, A., 2012. The effects of atorvastatin therapy on rheological characteristics of erythrocyte membrane, serum lipid profile and oxidative status in patients with dyslipidemia. J. Membr. Biol. 245, 697–705.

van Zwieten, R., Bochem, A.E., Hilarius, P.M., van Bruggen, R., Bergkamp, F., Hovingh, G.K., Verhoeven, A.J., 2012. The cholesterol content of the erythrocyte membrane is an important determinant of phosphatidylserine exposure. Biochim. Biophys. Acta 21 (12), 1493–1500.

Wang, J., Zhu, R., Sun, X., Zhu, Y., Liu, H., Wang, S.L., 2014. Intracellular uptake of etoposide-loaded solid lipid nanoparticles induces an enhancing inhibitory effect on gastric cancer through mitochondria-mediated apoptosis pathway. Int. J. Nanomedicine. 20 (9), 3987–3998.

Wen, Z.S., Liu, L.J., Qu, Y.L., Ouyang, X.K., Yang, L.Y., Xu, Z.R., 2013. Chitosan nanoparticles attenuate hydrogen peroxide-induced stress injury in mouse macrophage RAW264.7 cells. Mar. Drugs 11 (10), 3582–3600.

Xia, W. et al, 2010. Biological activities of chitosan and chitooligosaccharides. Food Hydrocolloids. http://dx.doi.org/10.1016/j.foodhyd.2010.03.003.

Yadav, A., Lomash, V., Samim, M., Flora, S.J., 2012. Curcumin encapsulated in chitosan nanoparticles: a novel strategy for the treatment of arsenic toxicity. Chem. Biol. Interact. 199 (1), 49–61, Jul 30.

Yuan 1, Z.X., Li, J.J., Zhu, D., Sun, X., Gong, T., Zhang, Z.R., 2011. Enhanced accumulation of low-molecular-weight chitosan in kidneys: a study on the influence of N-acetylation of chitosan on the renal targeting. J. Drug. Target. 19 (7), 540–551.

Zhang, C.M., Yu, S.H., Zhang, L.S., Zhao, Z.Y., Dong, L.L., 2014. Effects of several acetylated chitooligosaccharides on antioxidation, antiglycation and NO generation in erythrocyte. Bioorg. Med. Chem. Lett. 24 (16), 4053–4057. Aug 15.

Zhang, Z., Bu, H., Gao, Z., Huang, Y., Gao, F., Li, Y., 2010. The characteristics and mechanism of simvastatin loaded lipid nanoparticles to increase oral bioavailability in rats. Int. J. Pharm. 394 (1–2), 147–153.

Ziemba, B., Matuszko, G., Bryszewska, M., Klajnert, B., 2012. Influence of dendrimers on red blood cells. Cell. Mol. Biol. Lett. 17 (1), 21–35.

Please cite this article in press as: Harisa, G.I. et al., Influence of pravastatin chitosan nanoparticles on erythrocytes cholesterol and redox homeostasis: An *in vitro* study. Arabian Journal of Chemistry (2015), http://dx.doi.org/10.1016/j.arabjc.2015.10.016